



**HAL**  
open science

## Metabolic, cellular and defense responses to single and co-exposure to carbamazepine and methylmercury in *Dreissena polymorpha*

Clément Baratange, Séverine Paris-Palacios, Isabelle Bonnard, Laurence Delahaut, Grandjean Dominique, Laurence Wortham, Stéphanie Sayen, Andrea Gallorini, Jean Michel, D Renault, et al.

### ► To cite this version:

Clément Baratange, Séverine Paris-Palacios, Isabelle Bonnard, Laurence Delahaut, Grandjean Dominique, et al.. Metabolic, cellular and defense responses to single and co-exposure to carbamazepine and methylmercury in *Dreissena polymorpha*. *Environmental Pollution*, 2022, 300, pp.118933. 10.1016/j.envpol.2022.118933 . hal-03575444

**HAL Id: hal-03575444**

**<https://hal.science/hal-03575444>**

Submitted on 15 Feb 2022

**HAL** is a multi-disciplinary open access archive for the deposit and dissemination of scientific research documents, whether they are published or not. The documents may come from teaching and research institutions in France or abroad, or from public or private research centers.

L'archive ouverte pluridisciplinaire **HAL**, est destinée au dépôt et à la diffusion de documents scientifiques de niveau recherche, publiés ou non, émanant des établissements d'enseignement et de recherche français ou étrangers, des laboratoires publics ou privés.

1 **Metabolic, cellular and defense responses to single and co-exposure to carbamazepine and**  
2 **methylmercury in *Dreissena polymorpha***

3 Baratange Clément<sup>1</sup>, Paris-Palacios Séverine<sup>1</sup>, Bonnard Isabelle<sup>1</sup>, Delahaut Laurence<sup>1</sup>, Grandjean  
4 Dominique<sup>2</sup>, Wortham Laurence<sup>3</sup>, Sayen Stéphanie<sup>4</sup>, Gallorini Andrea<sup>5</sup>, Michel Jean<sup>3</sup>, Renault David<sup>6,7</sup>,  
5 Breider Florian<sup>2</sup>, Loizeau Jean-Luc<sup>5</sup>, Cosio Claudia<sup>1</sup>

6

7 <sup>1</sup> Université de Reims Champagne-Ardenne, UMR-I 02 INERIS-URCA-ULH SEBIO, Unité Stress  
8 Environnementaux et BIOSurveillance des milieux aquatiques (SEBIO), BP 1039 F-51687 Reims Cedex,  
9 France.

10 <sup>2</sup> ENAC, IIE, Central Environmental Laboratory, Ecole polytechnique Fédérale de Lausanne (EPFL),  
11 Station 2, 1015 Lausanne, Switzerland.

12 <sup>3</sup> Inserm UMR-S-1250 P3Cell, Université de Reims Champagne-Ardenne, 51685 Reims Cedex 2.

13 <sup>4</sup> Université de Reims Champagne-Ardenne, Institut de Chimie Moléculaire de Reims (ICMR), UMR  
14 CNRS 7312, BP 1039, F-51687 Reims Cedex 2, France.

15 <sup>5</sup> Department F.-A. Forel for Environmental and Aquatic Sciences, and Institute for Environmental  
16 Sciences, University of Geneva, Boulevard Carl-Vogt 66, 1211 Geneva 4, Switzerland.

17 <sup>6</sup> University of Rennes, CNRS, ECOBIO [(Ecosystèmes, biodiversité, évolution)] - UMR 6553, Rennes,  
18 France.

19 <sup>7</sup> Institut Universitaire de France, 1 rue Descartes, 75231 Paris Cedex 05, France.

20

21 Corresponding author: [claudia.cosio@univ-reims.fr](mailto:claudia.cosio@univ-reims.fr)

22 **Abstract**

23 Carbamazepine (CBZ) and Hg are widespread and persistent micropollutants in aquatic  
24 environments. Both pollutants are known to trigger similar toxicity mechanisms, *e.g.* reactive oxygen  
25 species (ROS) production. Here, their effects were assessed in the zebra mussel *Dreissena*  
26 *polymorpha*, frequently used as a freshwater model in ecotoxicology and biomonitoring. Single and  
27 co-exposures to CBZ (3.9  $\mu\text{g}\cdot\text{L}^{-1}$ ) and MeHg (280  $\text{ng}\cdot\text{L}^{-1}$ ) were performed for 1 and 7 days.  
28 Metabolomics analyses evidenced that the co-exposure was the most disturbing after 7 days,  
29 reducing the amount of 25 metabolites involved in protein synthesis, energy metabolism, antioxidant  
30 response and osmoregulation, and significantly altering cells and organelles' structure supporting a  
31 reduction of functions of gills and digestive glands. CBZ alone after 7 days decreased the amount of  
32  $\alpha$ -aminobutyric acid and had a moderate effect on the structure of mitochondria in digestive glands.  
33 MeHg alone had no effect on mussels' metabolome, but caused a significant alteration of cells and  
34 organelles' structure in gills and digestive glands. Single exposures and the co-exposure increased  
35 antioxidant responses *vs* control in gills and digestive glands, without resulting in lipid peroxidation,  
36 suggesting an increased ROS production caused by both pollutants. Data globally supported that a  
37 higher number of hyperactive cells compensated cellular alterations in the digestive gland of mussels  
38 exposed to CBZ or MeHg alone, while CBZ+MeHg co-exposure overwhelmed this compensation after  
39 7 days. Those effects were unpredictable based on cellular responses to CBZ and MeHg alone,  
40 highlighting the need to consider molecular toxicity pathways for a better anticipation of effects of  
41 pollutants in biota in complex environmental conditions.

42 **Keywords:** bioaccumulation, bivalve, cellular compensation, oxidative stress, toxicity pathways

43

44

45

## 46 Introduction

47 Biomonitoring of freshwater ecosystems is useful to anticipate harmful effects of pollutants in  
48 aquatic biota. A current aim in stress biology is to combine endpoints at different levels of biological  
49 organization, molecular to individual, to gain a better vision of molecular toxicity pathways in the  
50 frame of the adverse outcome pathway theory (Brinke, 2017). This strategy also allows identifying  
51 early-warning responses, useful to anticipate undesired impacts on biota and mitigate pollutant  
52 effects. In the future, these tools could help avoid long and costly processes of remediation and as  
53 such will benefit a wide community. In this context, representative biota that is found widely in  
54 ecosystems are of special interest. The zebra mussel *Dreissena polymorpha* (Pallas, 1771) was  
55 identified as an interesting non-model species for freshwaters due to its abundance, its wide  
56 distribution, its sessile lifestyle and its filtering activity, which favors bioaccumulation of  
57 contaminants (Binelli et al., 2015; Louis et al., 2019; Prud'homme et al., 2020; Hani et al., 2021).  
58 Nonetheless, the physiology of *D. polymorpha* remains poorly known yet, limiting its efficient use in  
59 biomonitoring and ecotoxicology. A research priority is to gain a better understanding of the  
60 molecular toxicity pathways of pollutants in this promising model to improve the analysis of its  
61 responses in complex exposure scenarios and *in situ*.

62 The antiepileptic drug carbamazepine (CBZ) is a personal and pharmaceutical care product  
63 (PPCP). CBZ is widely found in aquatic ecosystems due to its high consumption and poor elimination  
64 by wastewater treatment plants (Celiz et al., 2009; Clara et al., 2004). CBZ was measured from <1  
65 ng·L<sup>-1</sup> to 10 µg·L<sup>-1</sup> in freshwaters (Sacher et al., 2001; Miao et al., 2005; Metcalfe et al., 2009; Calisto  
66 et al., 2011), and concentrations are expected to increase due to its persistence and high human  
67 consumption (Oldenkamp et al., 2019). At the European level, no legislation for CBZ in the aquatic  
68 environment is established yet, but an environmental quality standard (EQS) of 0.5 µg·L<sup>-1</sup> was  
69 recommended (Kase, 2010; ETOX, 2011; Moermond, 2014). In bivalves, CBZ triggers oxidative stress,  
70 defense responses, but also an alteration of the energy metabolism, genotoxicity and reprotoxicity  
71 (Martin-Diaz et al., 2009; Chen et al., 2014; Aguirre-Martínez et al., 2015; Almeida et al., 2015;  
72 Brandts et al., 2018; Magniez et al., 2018; Franzellitti et al., 2019). However, the precise molecular  
73 toxicity targets of CBZ remain unknown.

74 Hg is a persistent and widespread pollutant in aquatic ecosystems. This metal is considered as a  
75 priority pollutant in Europe (Directive 2008/105/EC) and by the Minamata international convention  
76 (Reg. EC 1881/2006). In Europe, the current EQS for Hg is 70 ng·L<sup>-1</sup>. In aquatic ecosystems,  
77 methylmercury (MeHg) is biomagnified in food chains (Kershaw and Hall, 2019) and shows a lower  
78 depuration than inorganic mercury (IHg) in biota (Beauvais-Flück et al., 2017; Metian et al., 2020). In

79 bivalves, IHg causes oxidative stress, defense responses, alteration of the energy metabolism,  
80 disturbances of protein translation and genotoxicity (Franzellitti and Fabbri, 2006; Liu et al., 2011a,  
81 2011b; Navarro et al., 2011, 2012; Pytharopoulou et al., 2013; Jaumot et al., 2015; Velez et al., 2016;  
82 Coppola et al., 2017). Previous studies suggest that MeHg has different molecular toxicity pathways  
83 than IHg in biota, highlighting the need of assessing its impact in more detail for a better anticipation  
84 of risks it poses to ecosystems (Beauvais-Flück et al., 2017; Yang et al., 2020). Nonetheless, few  
85 studies focused on MeHg toxicity in bivalves (Gagnaire et al., 2004; Franzellitti and Fabbri, 2006;  
86 Parisi et al., 2021).

87 Scarce studies assessed toxic effects of co-exposure to ubiquitous pollutants, such as metals and  
88 organic pollutants (*e.g.* Almeida et al., 2018). CBZ and MeHg were selected here, because they are  
89 likely to be co-present in aquatic ecosystems (Andreu et al., 2016). Because CBZ and MeHg trigger  
90 similar cellular toxicity pathways, we hypothesized that their co-exposure would cause higher effects  
91 than single exposures. Here, metabolomic was analyzed in whole soft tissues to assess the  
92 phenotype at the individual level in *D. polymorpha*. In gills and digestive glands, histological and  
93 cytological analyses were performed, and lipid peroxidation, antioxidant and defense responses  
94 measured. The digestive gland is the organ where pollutants accumulate in higher concentrations,  
95 while gills are the most exposed organs to the environment. These two tissues are therefore highly  
96 relevant for the analysis of early cellular and molecular effects (Cardoso et al., 2013; Faggio et al.,  
97 2018). As such, this study aimed at answering the following questions: (i) which molecular toxicity  
98 pathways were induced by CBZ and MeHg? (ii) Does the co-exposure to CBZ and MeHg causes more  
99 effects than single exposures? (iii) Is there a link between observed effects and the bioaccumulation?

100

## 101 **Materials and methods**

### 102 *Exposures*

103 Individuals of *Dreissena polymorpha* were collected in the Der Lake (France; 48°36'22.02"N,  
104 4°46'34.0"E) in October 2019, transported to the laboratory, cleaned, selected by size (22-28 mm)  
105 and kept in water continuously aerated (82% O<sub>2</sub>) at the field temperature (14°C). Individuals were  
106 depurated for 7 days in 6 L of spring water (Cristaline Aurèle, table A1). For acclimation and to allow  
107 byssal fixation, 40 individuals per aquarium were transferred to 8 aquaria containing 3 L of spring  
108 water during 7 supplemental days. Animals were fed twice a week with a mixture of 50% *Chlorella*  
109 *vulgaris* and 50% *Scenedesmus spp.* using 2 million algae cells·day<sup>-1</sup>·individual<sup>-1</sup> and water was  
110 renewed 24 h after feeding. Histological analysis of gonads showed a post-spawning pattern (Figure  
111 A1). Four exposures were conducted in 2 aquaria each: (1) control, (2) CBZ (3.9±0.6 µg·L<sup>-1</sup>), (3) MeHg

112 (280±20 ng·L<sup>-1</sup>) and (4) co-exposure. Effective concentrations for CBZ and MeHg corresponded to 8x  
113 German EQS for CBZ (ETOX, 2011) and 4x European EQS for Hg (Directive 2008/105/EC).  
114 Temperature and feeding were identical to those during acclimation, but water was renewed daily.  
115 At D1, 2.50±1.02% of mussels died in the four aquaria, while 1.25±1.25% died at D7 in the four other  
116 aquaria. No significant differences were observed between exposures, thus mortality appeared  
117 negligible and unrelated to exposures.

118 For each exposure condition, mussels were sampled in one aquarium after 1 day (D1) and in  
119 the other aquarium after 7 days (D7). To mimic an active biomonitoring strategy (Louis et al., 2020),  
120 Individuals were elected as a replicate unit (Vaux et al., 2012) because of a high biological variability  
121 in this species (Pain Devin et al., 2014). This method ensured each individual had identical exposure  
122 conditions, hence limiting the impact of physiological and environmental conditions on toxicological  
123 effects and responses due to the pollutant (*e.g.* Louis et al., 2019). For bioaccumulation, whole soft  
124 tissues of nine animals were deshelled, rinsed with spring water and frozen at -80°C. For  
125 metabolomics, eight intact mussels were snap-frozen in liquid nitrogen and stored at -20°C. Histo-  
126 and cytological analyses were performed on three to nine animals sampled at D7. For gene  
127 expression and biochemical analyses, digestive glands and gills of eight mussels were dissected, snap-  
128 frozen in liquid nitrogen and stored at -80°C. Water aliquots (10 mL) were filtered (0.45 µm)  
129 immediately after the daily water renewal. First day samples were analyzed for the 1-day-long  
130 exposures, and other samples taken daily were pooled to analyze the average concentration of 7-  
131 day-long exposures. Water samples were frozen at -20°C for CBZ and acidified to 0.5% HCl and kept  
132 at 4°C for MeHg. Temperature, pH, conductivity, oxygen concentration, and nitrate, nitrite,  
133 ammonium concentrations were measured in a 40 mL aliquot before the daily water renewal with a  
134 multimeter and by spectrophotometry following Permachem protocol, respectively.

135

### 136 *CBZ and MeHg analysis*

137 Water aliquots were enriched 10x through centrifugal vacuum evaporation at 37°C using a  
138 Genevac HT Series (SP Scientific). The CBZ concentration in water was quantified using a High-  
139 Performance Liquid Chromatography (HPLC) system (Agilent technologies, 1260 Infinity), consisting  
140 of a quaternary pump and a photodiode array detector. A mobile phase containing acetonitrile (A),  
141 and ultra-pure water (ALPHA Q 18.2 MΩ·cm<sup>-1</sup>) with 0.1% orthophosphoric acid (B), was used to elute  
142 the analytes (20 µL injection volume) on a reverse-phase Agilent Pursuit XRs 5 C<sub>18</sub> column (5  
143 µm×250×3 mm) at 20°C. The elution was carried out at a flow rate of 0.80 mL·min<sup>-1</sup> with a gradient  
144 from 35/65% to 100/0% (v/v) A/B, and CBZ was detected at 214 nm.

145 The CBZ concentration in mussels was measured in freeze-dried and ground tissues,  
146 resuspended in 10 mL acetonitrile, 200  $\mu\text{L}$  n-heptane and 2.5 mL ammonium acetate (0.4 M). After  
147 centrifugation (1620 g 10 min), the supernatant was recovered, concentrated by a nitrogen flux  
148 evaporation at 40 °C and resuspended in 95% ultrapure water, 5% methanol and 0.1% formic acid  
149 (eluent A). Samples of 10  $\mu\text{L}$  were injected and analyzed by ultra-performance liquid-chromatography  
150 tandem mass spectrometry UPLC MS/MS (Acquity UPLC<sup>®</sup> Xevo TQ-MS system, Waters). A total  
151 running time of 15 min at 0.4 mL·min<sup>-1</sup> was performed with a gradient of 8 min 95% eluent A and 5%  
152 eluent B (95% methanol, 5% ultrapure water and 0.1% formic acid), 4 min 5% eluent A and 95%  
153 eluent B, 3 min 95% eluent A and 5% eluent B. The CBZ concentration in mussels was determined  
154 using a standard curve of 0.5, 1, 2, 3, 6 and 12 ng mL<sup>-1</sup> CBZ, and by adding an internal standard of  
155 deuterated CBZ at 50 ng mL<sup>-1</sup>. The CBZ recovery of pretreatment method was determined at 79±8%  
156 (n = 3). The analytical quality was verified by analyzing blanks. LOD of 6.8  $\mu\text{g kg}^{-1}$  dw was calculated.

157 MeHg concentration in water aliquots and mussels were analyzed by MERX-M (Brooks Rand  
158 Instruments). Mussel whole soft tissues were freeze-dried, ground and digested in 30% v/v HNO<sub>3</sub> at  
159 60°C for 12h prior MeHg analysis. MeHg concentration in mussels was determined using a standard  
160 curve of 0.5, 1, 2, 10, 50, 250, 500 and 1000 pg MeHg. The analytical quality was verified by analyzing  
161 certified reference material (DORM-4; NRC – CNRC) and blanks. MeHg recovery was determined at  
162 100±12% (n = 3), and LOD of 0.016 ng MeHg was calculated.

163

#### 164 *Targeted metabolomics*

165 Whole individuals were freeze-dried, shells were removed, and soft tissues were weighed,  
166 and homogenized into a 900  $\mu\text{L}$  mixture of methanol/chloroform (2/1, v/v). The samples were kept at  
167 -20°C overnight before adding 600  $\mu\text{L}$  of ultrapure water. The samples were vortexed and centrifuged  
168 at 4000 g (10 min 4 °C). The upper phase was collected and kept at -20°C until analyzed. Aliquots of  
169 120  $\mu\text{L}$  (>90 mg dw), 180  $\mu\text{L}$  (50-90 mg dw) or 220  $\mu\text{L}$  (<50 mg dw) were vacuum-dried at 32°C,  
170 resuspended in 30  $\mu\text{L}$  of methoxyamine hydrochloride (25 mg·L<sup>-1</sup>) in pyridine and shook at 40°C for  
171 60 min. Then, 30  $\mu\text{L}$  of N-methyl-N-(trimethylsilyl) trifluoroacetamide was added. After 60 min  
172 incubation at 40°C, 1  $\mu\text{L}$  of the sample was injected into the GC/MS as described by Thiébaud et al.  
173 (2021). After data acquisition, the chromatograms were deconvoluted and analyzed with  
174 MassHunter (MS Quantitative Analysis, Quant-My-Way, Agilent). Standard samples, containing 62  
175 reference compounds at 1, 2, 5, 10, 20, 50, 100, 200, 500, 750, 1000, and 1500  $\mu\text{M}$  allowed the  
176 quantification of 31 metabolites by quadratic calibration (tables A2, A3 and A4), including sugars,  
177 amino acids, polyols, organic acids. This approach allowed covering the main metabolic pathways.

178

179 *Histology and cytology*

180 For histopathology, gonads, gills and digestive glands were fixed in Bouin's aqueous  
181 solution for 24 h immediately after dissection at D7. Dehydration was performed by successive  
182 alcohol baths from 50 to 100°, and samples were placed in butanol for at least 24 h to permeate all  
183 tissues. Samples were impregnated with hot paraffin and embedded by cooling (Paris-Palacios et al.,  
184 2000, 2003). Sections (5 µm) were obtained from a Leica microtome, stained with nuclear fast red  
185 (NR) and picro-indigo-carmin (PIC) and mounted on glass slides for light microscopy. Gender and  
186 gonadic reproductive stage of mussels were determined according to Louis et al. (2020). Three  
187 sections of each mussel were observed for the assessment of the frequency and the intensity of  
188 potential pathologies resulting from exposures (adapted from Jaffal et al., 2015 and Jacquin et al.,  
189 2019) and scored (table A5). A global score of histological perturbations was calculated as the  
190 median value of all scores. Mussels presenting parasite(s) weren't analyzed.

191 For cytology, a piece of the digestive gland was sampled from three mussels for each  
192 exposure at D7, immediately cryofixed with an EM ICE High pressure freeze (LEICA) and stored in  
193 liquid nitrogen. Then, 100 nm thick cryosections were freeze-dried, observed with an electronic  
194 microscope (JEM - 2100F; JEOL) and image capture were performed with a Digital Micrograph GMS3  
195 (GATAN). The sensitivity of this system allows observations without any contrasting product.  
196 Mitochondria in cells of digestive glands were counted and classified into different categories (figure  
197 A2). Endoplasmic reticula were also analyzed, and a score was determined based on the frequency  
198 and severity of alterations.

199

200 *Gene expression level*

201 RNA was extracted with TRI Reagent following Euromedex protocol. Reverse transcription  
202 was performed at 42°C for 1 h followed by 3 min at 95°C using the verso cDNA synthesis kit on 400 ng  
203 RNA with oligodT primers according to the Thermo Scientific protocol. Quantitative polymerisation  
204 chain reactions (qPCR) were performed with the Absolute Blue qPCR SYBR Green kit (Thermo  
205 Scientific) on 3 µL of 1/10 dilution of cDNA reaction, using a CFX96 automaton (BioRad), 15 min at  
206 95°C, followed by 40 cycles of 10 sec at 95°C and 45 sec at 60°C. Relative gene expression levels of  
207 catalase (cat), glutathione-s-transferase (gst), superoxide dismutase (sod) and metallothionein (mt;  
208 table A6) were calculated following the  $2^{-\Delta\Delta Ct}$  method, using actin (act) and ribosomal protein S3 (ps3)  
209 as reference genes (Schmittgen and Livak, 2008).



210

211 *Enzyme activities and lipid peroxidation*

212 Each individual was weighed, ground (8/1 v/w) in 50 mM phosphate buffer pH 7.4, 1 mM  
213 phenylmethylsulfonyl fluoride and 1 mM L-serine borate as protease inhibitors. After 15 min at 3000  
214 g (4 °C), the supernatant (= homogenate) was collected and kept at -80°C.

215 The automated spectrophotometer Gallery (Thermo Scientific) served for the determination  
216 of protein concentration, GST activity (Garaud et al., 2016) and lipid hydroperoxide (LOOH)  
217 concentration resulting from lipid peroxidation (Arab and Steghens 2004). Protein concentration to  
218 normalize enzyme activities was measured at 600 nm after 5 min in 1/7 (v/v) of the homogenate by  
219 colorimetric method of red pyrogallol, with bovine serum sCal (66.7  $\mu\text{g}\cdot\text{L}^{-1}$ ) for calibration and protein  
220 reagents U/CSF from the manufacturer, diluted 50 to 200x (Thermo Scientific). GST activity was  
221 measured at 340 nm for 4 min in 1/40 (v/v) of the homogenate by colorimetric method with 0.9 mM  
222 1-chloro-2,4-dinitrobenzene, 1 mM reduced glutathione in 0.1 M phosphate buffer pH 6.5. LOOH was  
223 measured at 620 nm after 30 min in 1/46 (v/v) of the homogenate with 139 mM Fe II D-gluconate  
224 dihydrate, 240 mM orange xylenol in an acidic solution ( $\text{H}_2\text{SO}_4$  40 mM, glycerol 1.37 M, formic acid  
225 20 mM and NaCl 0.9%), using a calibration curve from tert-butyl hydroperoxide at 0.125, 0.25, 0.5, 1,  
226 2, 4, 8 and 16  $\mu\text{M}$ .

227 CAT activity (Beer and Sizer 1952) was measured in the linear range of the reaction at 240  
228 nm for 120 sec in 1/100 (v/v) of the homogenate by a spectrophotometer (Cary 50, Agilent) with 14  
229 mM hydrogen peroxide in 50 mM phosphate buffer pH 7.4, using a calibration curve from purified  
230 bovine serum CAT at 1.25, 2.5, 5, 10, 15 and 20  $\text{U}\cdot\text{mL}^{-1}$ .

231 SOD activity (Paoletti et al., 1986) was measured in the linear range of the reaction after 20  
232 min in darkness, at 340 nm for 30 min in 1/85 (v/v) of the homogenate by a spectrophotometer  
233 (Spark 10M, TECAN) with 0.1 M EDTA, 0.05 M  $\text{MnCl}_2$ , 10 mM  $\beta$ -mercaptoethanol, 7.5 mM NADH in 50  
234 mM phosphate buffer pH 7.4. Concentrations were determined using a calibration curve from  
235 purified bovine serum SOD at 0.125, 0.25, 0.35, 0.5 and 0.7  $\text{U}\cdot\text{mL}^{-1}$ .

236

237 *Data interpretation and statistical analysis*

238 Data were presented as mean $\pm$ standard error of the mean (SEM). Homoscedasticity and  
239 normality of values, and/or residuals, were verified by Bartlett's tests and Kolmogorov-Smirnov's

240 tests in Rstudio software (v 4.0.3.;  $\alpha=5\%$ ). Student tests vs control were applied if these criteria were  
241 met, while Wilcoxon-Mann-Whitney tests vs control were applied if not ( $\alpha=5\%$ ).

242 For metabolomics data, p-values obtained from Student or Wilcoxon-Mann-Whitney tests  
243 were corrected through positive false discovery rate (pFDR) procedure (Storey and Tibshirani 2003;  
244 Storey 2015) using *cp4p* package. Metabolites were considered as significantly different when p-  
245 value was  $<0.05$  and fold change (FC) values  $>1.5$  vs respective control. Metabolites significantly  
246 modified were analyzed in Metaboanalyst (<http://www.metaboanalyst.ca>) with the KEGG database  
247 (October 2019). Heat maps were constructed in Genesis (Sturn et al., 2002) comparing  $\log_2$ -  
248 transformed FC normalized by control.

249 The bioaccumulation factor (BAF;  $L\cdot kg^{-1}$ ) was calculated dividing pollutant concentration in  
250 mussels by effective concentration of the pollutant in water. To describe responses, the term  
251 synergism, neutral and antagonism were used when the response was higher, similar or lower for the  
252 co-exposure than the sum of the individual responses, respectively.

253

## 254 **Results**

### 255 *Water parameters*

256 Concentrations of CBZ ( $3.9\pm 0.6 \mu g\cdot L^{-1}$ ) and MeHg ( $280\pm 20 ng\cdot L^{-1}$ ) were stable among  
257 exposures ( $n = 4$ ). Physico-chemical parameters measured from water samples were also stable and  
258 similar among exposures: pH  $8.41\pm 0.02$ , conductivity  $530\pm 30 \mu S\cdot cm^{-1}$ , oxygen saturation  $78.1\pm 0.4\%$   
259  $O_2$ , nitrate  $9.7\pm 0.6 mg\cdot L^{-1}$ , nitrite  $0.10\pm 0.01 mg\cdot L^{-1}$ , ammonium  $0.19\pm 0.03 mg\cdot L^{-1}$  and temperature  
260  $13.7\pm 0.1^\circ C$  (figure A3). As water physico-chemical parameters were similar among exposures from  
261 D1 to D7, all the observed responses could be attributed to the impact of pollutants.

262

### 263 *CBZ and MeHg bioaccumulation*

264 CBZ bioaccumulation (figure 1) was similar between single and co-exposures both at D1 and  
265 D7, showing a BAF of  $35\pm 1$ . Compared to the control mussels, MeHg concentration increased 12x at  
266 D1 and 63x at D7 in MeHg single exposure, resulting in a BAF of 755 and 3973, respectively. In co-  
267 exposure, MeHg bioaccumulation increased 23x at D1 and 109x at D7 vs controls, resulting in a BAF  
268 of 1471 and 6973, respectively, but showing no statistical difference with single exposure. As such  
269 responses were neutral for bioaccumulation and data highlighted a 20-40x and 100-200x higher BAF  
270 of MeHg than CBZ in mussel tissues at D1 and D7, respectively. No bioaccumulation of the other

271 pollutant was measured in single exposures. MeHg concentration in controls reached  $0.017 \pm 0.003$   
272  $\text{mg} \cdot \text{kg}^{-1}$  confirming clean exposure conditions.

273

#### 274 *Targeted metabolomics*

275 Metabolites characterized *D. polymorpha* phenotype at the individual level (Figure 2, table  
276 A2 and A3). Only the co-exposure at D7 significantly impacted the metabolome resulting in the  
277 decrease of 25 metabolites, involved in 16 metabolic pathways of amino acids, energy metabolism  
278 and antioxidant responses (table 1). CBZ exposure at D7 decreased 2.2x the concentration of  $\alpha$ -  
279 aminobutyric acid, involved in cysteine and methionine metabolism. MeHg single exposure and all D1  
280 exposures didn't modulate metabolites significantly. Synergism was observed for metabolomics at D7  
281 when comparing co-exposure with single exposures and were congruent with the higher  
282 bioaccumulation observed at D7 vs D1 for MeHg, while CBZ bioaccumulation was similar.

283

#### 284 *Histology and cytology*

285 To further understand metabolomic observations at D7, we compared histopathology of gills  
286 and digestive glands, because of their direct exposure to the media and detoxifying role in bivalves,  
287 respectively (table 2; figures 3 and A4). Exposure to MeHg and the co-exposure caused a high degree  
288 of gill fibrosis, deformation, and alteration: 25 to 50% of the gills respiratory surface was altered.  
289 Besides, 20 to 40% of digestive tubules showed numerous fibrosis and cell alterations, such as  
290 picnotic nucleus, in progress and terminal lysis or necrosis. Because of involution and atresia, 10 to  
291 20% of digestive tubules appeared non-functional. In these exposures, the infiltration of immune  
292 cells and an accumulation of liquid in the tissue evoked edema inflammatory process. As such,  
293 alterations observed in gills and digestive glands likely resulted in a reduction of function of those  
294 organs. For comparison, control and CBZ caused few alterations in gills and no significant alteration  
295 in digestive glands. Responses were neutral for histopathology when comparing the co-exposure  
296 with single exposures. Histopathology was congruent with metabolomics for the co-exposure and  
297 CBZ exposure, but not for MeHg exposure, as MeHg had significant cellular effects unreflected in  
298 metabolomics.

299 In line with histopathology data, cytology in digestive glands pointed MeHg exposure and co-  
300 exposure to result in most cells having high grades of alterations, while other cells presented an  
301 ultrastructure evoking high metabolic capacity (figures 3 and A4). These cells presented a higher  
302 amount of reticulum and mitochondria than healthy cells from control mussels, a large well

303 conformed nucleus and nucleolus and no alteration of organelles or membranes, thus these cells  
304 were qualified as “hyperactive” cells. The altered cell type presented few and deformed reticulum,  
305 mitochondria and nuclei likely related to a low metabolic capacity. More in detail, mitochondrial  
306 alterations significantly increased vs control with mitochondrial bodies, cristae malformation or  
307 break, inner and outer membrane impairment. Moreover, reticulum cisternae were largely dilated. A  
308 reduction of the amount of cisterna and some breaks and dispersion were also observed (figures 3  
309 and A2). Erosion of cilia, and modification of membrane form or thickness in cytoplasmic and nuclear  
310 regions was sometimes observed. Exposure to CBZ also resulted in two types of digestive cells:  
311 hyperactive and altered cells as described above. The amount of altered type cells in CBZ-exposed  
312 mussels varied highly among areas of the digestive gland and among individuals masking any obvious  
313 trend. Few cells also appeared hyperactive with important alterations, *i.e.* presenting both types. In  
314 control, 83% of digestive cells showed ultra-structural patterns typical from healthy cells, *i.e.* without  
315 pathology. Only 10±4% non-functional mitochondria and a large amount of well-conformed  
316 reticulum cisterns were observed. Responses were neutral for cytology when comparing the co-  
317 exposure with single exposures. Cytology was congruent with histopathology for the co-exposure  
318 and MeHg exposure, but not for CBZ exposure. These observations together with metabolomics  
319 suggested that hyperactive cells efficiently compensated altered cells in MeHg and CBZ exposures,  
320 resulting in an unimpacted metabolome in single exposures, but a modified metabolome in the co-  
321 exposure.

322

### 323 *Oxidative stress and defences*

324 Because both CBZ and MeHg are expected to trigger ROS production, we analyzed oxidative  
325 stress and defense endpoints (figure 4). At the transcript level, CBZ significantly upregulated 1.7 and  
326 1.9x mt gene in gills and digestive glands respectively at D1, and 1.8x sod gene in gills at D7, while it  
327 increased 1.4x CAT activity in digestive glands at D7. MeHg significantly upregulated 1.8x cat at D1  
328 and 2x sod at D7 in gills and increased 1.6x and 1.2x SOD activity in gills and digestive glands  
329 respectively at D7. Co-exposure also upregulated 2x mt expression in digestive glands at D1 and  
330 increased 1.5x SOD activity and 1.5x CAT activity in gills at D7. GST activity or LOOH concentration  
331 wasn't significantly modified here. Data suggested a ROS production by CBZ and MeHg in gills and the  
332 digestive gland, suggesting an antagonism on these endpoints in the co-exposure, except for mt gene  
333 expression and SOD activity that were neutral. Effects globally suggested different responses in  
334 organs depending on the pollutant and no obvious correlation with bioaccumulation.

335

## 336 Discussion

### 337 CBZ exposure

338 Data here suggested that CBZ alone triggered a low stress level. At D7, cytology of digestive  
339 glands revealed (i) the occurrence of cells defined as “hyperactives”, with ultrastructure typically  
340 linked to an increased metabolism (e.g. higher amount of endoplasmic reticulum, mitochondria and  
341 nucleus size higher than control), and (ii) the occurrence of other cells with cytological features of a  
342 reduced metabolism and an important rate of alterations (e.g. broken cristae in mitochondria,  
343 abnormal nucleus). Concomitantly few damages were observed at the tissue level by histopathology.  
344 The link between the ultrastructure of cells and its functions was fully demonstrated by others in  
345 most types of cells (Segner and Braunbeck, 1990, 1998; Biagianti-Risbourg, 1997). Ultrastructural  
346 perturbations were recognized as a biomarker of interest in ecotoxicology (Segner and Braunbeck,  
347 1990, 1998; Biagianti-Risbourg, 1997). Few studies focused on structure and ultrastructure of cells in  
348 bivalves, and to our knowledge no studies investigated CBZ effect at the cytological level (Au et al.,  
349 2004). A juxtaposition of cells showing important alterations, and cells showing indications of  
350 increased activity (forming a mosaic), was also reported in the liver of fish exposed to copper and  
351 procymidone (Paris-Palacios et al., 2000; Paris-Palacios et al., 2003). Authors suggested a  
352 compensation of damaged cells by “hyperactive” cells (Paris-Palacios et al., 2000; Paris-Palacios et al.,  
353 2003). Similarly, here, damages observed in altered cells appeared efficiently compensated by the  
354 increased metabolic activity of the “hyperactive” cells. Consequently, the metabolome was efficiently  
355 maintained, except for the significant decrease of  $\alpha$ -aminobutyric acid amount at D7. In *Daphnia*  
356 *magna* exposed 48h to 1.75 to 14 mg·L<sup>-1</sup> CBZ, a significant decrease by 3 to 15% of alanine, glycine,  
357 leucine, proline, serine and tryptophan concentrations, suggested an increase of protein biosynthesis  
358 and amino acid metabolism (Kovacevic et al., 2016). In the same line, in 96h post-fertilization larvae  
359 of *Danio rerio*, 24h exposure to 3.54  $\mu$ g·L<sup>-1</sup> CBZ mainly reduced amino acids (Huang et al., 2016).  
360 Nonetheless, studies were performed at high CBZ concentrations for the former, and for the latter in  
361 juveniles who are more sensitive than adults (Huang et al., 2016; Huang et al., 2017), limiting a direct  
362 comparison with our experimental conditions. Besides, here CAT activity increased in digestive glands  
363 at D7, without lipid peroxidation, supporting that cellular defenses copped well ROS production by  
364 CBZ. For comparison, in *Scrobicularia plana*, a 96h exposure to 3  $\mu$ g·L<sup>-1</sup> CBZ reduced CAT and SOD  
365 activities 1.5x in soft tissues, and increased 1.3x lipid peroxidation (Freitas et al., 2015), suggesting  
366 that *D. polymorpha* might be more tolerant than *S. plana* thanks to an efficient defense response. In  
367 the same line, here the mt gene was upregulated in gills and digestive glands at D1. MT is mainly  
368 known for its role in metal detoxification but was also described as a ROS scavenger and suspected to  
369 have an anti-apoptotic function (Takahashi, 2012). MT content increased 10x in liver of fish *Rutilus*

370 *rutilus* exposed 4 days to 200  $\mu\text{g}\cdot\text{L}^{-1}$  of the fungicide procymidone (Paris-Palacios et al., 2003). As  
371 such, MT might be involved in tolerance against ROS in *D. polymorpha* in our experimental  
372 conditions.

373

#### 374 *MeHg exposure*

375 Here, MeHg exposure, similarly to CBZ exposure, resulted in cellular damages without impact  
376 on the metabolome, supporting that *D. polymorpha* could cope with this stress level thanks to an  
377 efficient defense response. Indeed, no metabolite was modulated, while numerous necrosis, altered  
378 cells and degenerative alterations in gills and digestive glands such as ciliary erosion, cell necrosis and  
379 tissue malformations were observed. The inflammation by Hg was previously reported in bivalves in  
380 several histopathological studies (Bigas et al., 2006; Cappello et al., 2013; Chalghmi et al., 2016; do  
381 Amaral et al., 2019). It is considered as nonspecific consequences of physiological adaptation to a  
382 stress (Bigas et al., 2006; Cappello et al., 2013; Chalghmi et al., 2016; do Amaral et al., 2019).  
383 However, cytological observations here evidenced altered digestive cells, showing damaged  
384 membranes and mitochondria. Concomitantly, we observed an increased number of cells presenting  
385 a high number of mitochondria and a development of their REG, pointing to a high metabolic activity,  
386 likely compensating the loss of activity of damaged cells. Similarly, exposure of *Anguilla anguilla* 11  
387 days to 50  $\text{ng}\cdot\text{L}^{-1}$  MeHg, upregulated (10-500x) genes *cox1* and *12s* involved in mitochondrial  
388 metabolism, while altered mitochondria were likely compensated by an increased number of  
389 mitochondria observed in muscle fibers by electron microscopy (Claveau et al., 2015). Mitochondria  
390 are expected targets of MeHg in animals (Ferreira et al., 2018; Correa et al., 2020). For example,  
391 MeHg depolarized mitochondrial membrane in synaptosomes (Hare and Atchinson, 1992). Here,  
392 MeHg at D1 also upregulated *cat* gene expression level in gills and increased SOD activity in digestive  
393 glands. MeHg at D7, increased *sod* gene expression and SOD activity in gills. Data for MeHg  
394 supported a ROS production in tissues not resulting in lipid peroxidation and an efficient antioxidant  
395 response in our experimental conditions. An increase of intracellular ROS levels by 1.2 to 1.5x was  
396 previously reported in copepods *Tigriopus japonicus* and *Paracyclina nana* exposed to 1 to 1000  $\text{ng}\cdot\text{L}^{-1}$   
397 MeHg 24h, together with an increase of GST activity by 1.3 to 1.5x (Lee et al., 2017a; Lee et al.,  
398 2017b). Here, data globally suggested that MeHg induced cellular damage and altered organelle  
399 functions, but cellular compensation and defense responses resulted in tolerance in *D. polymorpha*  
400 to MeHg exposure.

401

#### 402 *Co-exposure*

403 Here, the co-exposure in *D. polymorpha* was the most disturbing for the metabolome at D7,  
404 and showed a synergistic response vs single exposures. In contrast to single exposures, in the co-  
405 exposure hyperactive cells didn't efficiently compensate for damaged cells, resulting in the reduction  
406 of 25 of the 31 quantified metabolites. Here, co-exposure also triggered ROS production as shown by  
407 increased mt gene expression level in digestive glands at D1, and CAT and SOD activities in gills at D7.  
408 Besides, a 2x decrease of glutamic acid and glycine supported glutathione biosynthesis at D7. Those  
409 responses suggested a higher ROS production for co-exposure than single exposures, in line with the  
410 known ability of both pollutants to trigger ROS production (Freitas et al., 2015; Lee et al., 2017a; Lee  
411 et al., 2017b). Nonetheless, lipid peroxidation wasn't measured here, which supported an efficient  
412 antioxidant response maintaining the RedOx balance of *D. polymorpha* in the co-exposure. However,  
413 the impact of the co-exposure at D7 wasn't predictable based on the low toxicity level triggered by  
414 single exposures. Similarly, in *Ruditapes philippinarum*, exposure 21 days to  $10 \mu\text{g}\cdot\text{L}^{-1}$  IHg and  $3 \mu\text{g}\cdot\text{L}^{-1}$   
415 benzo[a]pyrene resulted in synergistic effects on glutathione content and lipid peroxidation, while  
416 GST and CAT activities weren't modified by the co-exposure (Jiang et al., 2019). In contrast, in *R.*  
417 *philippinarum* exposure 7 days to  $10 \mu\text{g}\cdot\text{L}^{-1}$  IHg and  $25 \mu\text{g}\cdot\text{L}^{-1}$  microplastics caused antagonistic  
418 responses on histological alterations, and no modification of CAT activity, GSH content or lipid  
419 peroxidation in gills and digestive glands, compared to single exposures (Sikdokur et al., 2020).  
420 Although microplastics are a different type of pollutants likely having distinct modes of action, the  
421 number of studies investigating combined effects of pollutants is very low, limiting comparisons with  
422 the literature. Here, antioxidant defenses didn't seem directly related to pollutant bioaccumulation,  
423 cellular and metabolome impact. As such, data suggested that other molecular toxicity pathways  
424 triggered by the co-exposure could contribute to observed damages.

425 Modulated metabolites were further analyzed to identify additional putative molecular  
426 toxicity pathways occurring here. An alteration of tRNA-aminoacyl biosynthesis and the metabolism  
427 of several amino acids were observed, suggesting an impact on protein biosynthesis. For example,  
428 branched chain amino acids (BCAAs; isoleucine, leucine and valine) were decreased in line with  
429 observations in *D. magna* exposed 48h to  $1.75$  to  $14 \text{mg}\cdot\text{L}^{-1}$  CBZ (Kovacevic et al., 2016). BCAAs are  
430 known precursors for the synthesis of stress response proteins in aquatic invertebrates such as  
431 chaperon proteins that maintain molecular and cellular functionalities (Calder, 2006). Free amino  
432 acids are also known to be central for cell osmoregulation in mollusks (Viant et al., 2003, Kovacevic et  
433 al., 2016). The decreased concentrations of free amino acids in the co-exposure here might suggest  
434 an osmotic stress of *D. polymorpha*. In adductor muscles of *R. philippinarum*, IHg decreased amino  
435 acid concentrations, which was likely compensated by an increase of other osmolytes such as  
436 betaine, homarine and taurine (Liu et al., 2011a). Similarly, the increase of amino acids in gills of *R.*

437 *philippinarum* was likely compensated by a decrease of these same osmolytes (Liu et al., 2011b). In  
438 both studies, authors hypothesized that IHg disturbed osmoregulation functions, potentially causing  
439 an osmotic stress. In the same line, an increase of osmolality, suggesting osmotic perturbation, was  
440 measured in the plasma of *Solea senegalensis* 48h after 1 mg·kg<sup>-1</sup> CBZ injection (González-Mira et al.,  
441 2016). Here, obvious alterations of gill filaments and digestive cells were observed in *D. polymorpha*  
442 in the co-exposure, which could result from osmoregulation disturbances together with ROS  
443 production. However, other analyses beyond the scope of the present work are needed to conclude.

444 Pathway analysis of metabolites also indicated an alteration of energetic and carbohydrate  
445 metabolism, such as galactose and pyruvate metabolism in *D. polymorpha* co-exposed to CBZ+MeHg.  
446 Similarly, cellular and mitochondrial alterations pointed to an alteration of functions essential for the  
447 energy metabolism (Rodrigo and Costa 2017; Faggio et al., 2018). Here, glucose, inositol and  
448 mannose, glyceric, fumaric and malic acids were significantly reduced, suggesting a higher energy  
449 consumption and an increased energy production through alternative pathways, such as the citric  
450 cycle. In aquatic invertebrates, stress is known to reshuffle metabolism, *i.e.* using amino acids to  
451 produce energy through an alternative pathway (Sokolova et al., 2012). At higher stress levels, the  
452 physiological homeostasis can be altered, eventually resulting in dysregulation of the metabolite  
453 fluxes in and among metabolic pathways. In *R. philippinarum*, exposed 48h to 20 µg·L<sup>-1</sup> IHg ATP/ADP  
454 ratio, succinic and citric acid decreased in adductor muscle, while ATP/ADP ratio, lactic acid and α-  
455 ketoglutarate increased in gills (Liu et al., 2011a; Liu et al., 2011b). Similarly, in *R. philippinarum*, 21  
456 days exposure to 2 µg·L<sup>-1</sup> IHg decreased 1.5x glycogen in hepatopancreas (Jiang et al., 2019). In *M.*  
457 *galloprovincialis*, exposure 96h to 6 µg·L<sup>-1</sup> CBZ decreased glycogen and protein contents 1.5 and 1.3x  
458 respectively, while the mitochondrial electron transport system (ETS) increased 1.2x (Oliveira et al.,  
459 2017). All these studies highlighted a high impact on the energy metabolism, evidenced by a high  
460 energy demand. It would be interesting to measure ETS in the future, as it could be a relevant  
461 indicator of metabolic capacity of mussels (Bielen et al., 2016). In sum, both CBZ and MeHg could  
462 alter energy metabolism, and have the potential to disrupt physiological homeostasis at high  
463 concentration individually. The co-exposure to CBZ+MeHg might result in a similar stress level than  
464 single exposures at a much higher concentration.

465

#### 466 *Bioaccumulation and observed effects*

467 Here, bioaccumulation of MeHg measured in *D. polymorpha* at D1 and D7 corresponded to  
468 values found at moderately (≤0.4 mg·kg<sup>-1</sup> dw) and highly contaminated sites (≤1.9 mg·kg<sup>-1</sup> dw),  
469 respectively. For comparison, MeHg concentration reached 0.4 mg·kg<sup>-1</sup> dw in *Cerastoderma glaucum*  
470 tissues (Dominik et al., 2014) and 0.21 mg·kg<sup>-1</sup> MeHg dw in *Crassostrea virginica* (Apeti et al., 2012) in



471 moderately contaminated sites. Besides, all values were  $<0.5 \text{ mg}\cdot\text{kg}^{-1} \text{ fw}$  (*i.e.*  $\sim 2.5 \text{ mg}\cdot\text{kg}^{-1} \text{ dw}$ ), the  
472 threshold for seafood commercialization in Europe (EC 1881/2006). For CBZ, a BAF of 37 was  
473 observed here. Similarly, a BAF of 25 was determined in *M. galloprovincialis* exposed 20 days to  $15.7$   
474  $\mu\text{g}\cdot\text{L}^{-1}$  CBZ (Serra-Compte et al., 2018). On the contrary, CBZ bioaccumulation was 10x lower in *D.*  
475 *polymorpha* after 1 to 6 months exposure to  $5 \mu\text{g}\cdot\text{L}^{-1}$  CBZ (Daniele et al., 2017; Magniez et al., 2018)  
476 and in bivalves sampled in polluted sites ( $\leq 11 \mu\text{g}\cdot\text{kg}^{-1} \text{ dw}$ ; Almeida et al., 2020). The latter studies  
477 didn't use an internal standard, while Serra-Compte et al. (2018) and here did, likely explaining those  
478 differences. Further analyses of environmental samples with internal standards are needed to  
479 conclude. Metabolites of CBZ (*e.g.* acridine, 2-hydroxy-CBZ) weren't analyzed here, because previous  
480 analysis in *D. polymorpha* suggested their absence after 1 to 6 months of exposure to  $5 \mu\text{g L}^{-1}$  CBZ  
481 (Magniez et al., 2018). Here we hypothesized that the drug parent was mainly causing biological  
482 effects.

483 Biological effects are generally expected to be linked with bioaccumulation (Sijm and Hermens,  
484 2001; Le Guernic et al., 2016; Kershaw and Hall, 2019). Here, bioaccumulation of MeHg in *D.*  
485 *polymorpha* increased from D1 to D7, while CBZ bioaccumulation was similar, but metabolome and  
486 defense responses weren't altered after single exposure. As such, bioaccumulation and biological  
487 responses didn't seem linearly correlated here. Since bioaccumulation of MeHg and CBZ were similar  
488 for all exposures at D7, data supported that CBZ and MeHg impacted similar molecular toxicity  
489 pathways. Previous studies also showed that bioaccumulation was unrelated to effects observed. For  
490 example, in *R. philippinarum*, co-exposure 21 days to  $2 \mu\text{g}\cdot\text{L}^{-1}$  IHg and  $3 \mu\text{g}\cdot\text{L}^{-1}$  benzo[a]pyrene caused  
491 lipid peroxidation, while single exposures didn't (Jiang et al., 2019). Besides, single exposures 28 days  
492 of *R. philippinarum* to  $1 \mu\text{g}\cdot\text{L}^{-1}$  CBZ and  $0.5 \mu\text{g}\cdot\text{L}^{-1}$  Cd caused lipid peroxidation and altered GST  
493 activity, while the co-exposure resulted in a similar bioaccumulation, but unaltered defense  
494 responses (Almeida et al., 2018). Contrasting responses in co-exposures underline the need to better  
495 understand the molecular toxicity pathways of pollutants in *D. polymorpha* to improve biomonitoring  
496 in complex environments, and anticipate effects.

497

## 498 **Conclusion**

499 Data presented here investigated the toxicity of CBZ and MeHg at 8x and 4x EQS concentrations,  
500 respectively in a freshwater bivalve. Single exposures didn't alter the metabolome despite an  
501 increased number of altered cells, likely compensated by hyperactive cells. This compensation didn't  
502 appear efficient enough for the co-exposure CBZ+MeHg at D7, resulting in a decrease of metabolites  
503 involved in RedOx, amino acid, osmoregulation and energy metabolism. We attributed these

504 responses to similar molecular toxicity pathways induced by CBZ and MeHg. However, such effects  
505 were unpredictable based on responses to single exposures, confirming the need to study more in  
506 detail molecular toxicity pathways. Indeed, co-exposure to pollutants should be better considered by  
507 the legislation and may well modify current EQS. Studies linking bioaccumulation and molecular  
508 toxicity pathways of pollutants at environmental concentrations are thus a research priority to better  
509 anticipate effects *in situ*. Further non-targeted analysis (e.g. proteomics, RNAseq) at the individual  
510 level and on specific organs will give supplemental clues on the involved molecular toxicity targets,  
511 and could help to identify early-warning responses.

512

### 513 **Acknowledgements**

514 We are grateful to the EcoChimie Platform (EcoChim) from UMS OSUR 3343 for access to  
515 metabolomics facilities and support. Authors would like to thank Fanny Louis, Olivier Fernandez and  
516 Nicolas Borie for their technical help. The authors also benefitted from the French GDR “Aquatic  
517 Ecotoxicology” framework which aims at fostering stimulating scientific discussions and  
518 collaborations for more integrative approaches.

519

### 520 **Funding**

521 This research was funded by Grand Reims through the Aquasurv Chair, by the French National  
522 program EC2CO (Ecosphère Continentale et Côtière) through the CARMA n°12837 program and by  
523 the SFR Condorcet through the DeMo program.

524

### 525 **References**

- 526 Aguirre-Martínez, G.V., DelValls, A.T., Martín-Díaz, L.M., 2015. Yes, caffeine, ibuprofen,  
527 carbamazepine, novobiocin and tamoxifen have an effect on *Corbicula fluminea* (Müller, 1774).  
528 Ecotoxicology and Environmental Safety 120, 142–154.  
529 <https://doi.org/10.1016/j.ecoenv.2015.05.036>
- 530 Almeida, Â., Freitas, R., Calisto, V., Esteves, V.I., Schneider, R.J., Soares, A.M.V.M., Figueira, E., 2015.  
531 Chronic toxicity of the antiepileptic carbamazepine on the clam *Ruditapes philippinarum*.  
532 Comparative Biochemistry and Physiology Part C: Toxicology & Pharmacology 172–173, 26–35.  
533 <https://doi.org/10.1016/j.cbpc.2015.04.004>
- 534 Almeida, Â., Calisto, V., Esteves, V.I., Schneider, R.J., Soares, A.M.V.M., Figueira, E., Freitas, R., 2018.  
535 Effects of single and combined exposure of pharmaceutical drugs (carbamazepine and  
536 cetirizine) and a metal (cadmium) on the biochemical responses of *R. philippinarum*. Aquatic  
537 Toxicology 198, 10–19. <https://doi.org/10.1016/j.aquatox.2018.02.011>
- 538 Almeida, Â., Esteves, V.I., Soares, A.M.V.M., Freitas R., 2020. Effects of Carbamazepine in Bivalves: A  
539 Review, Reviews of Environmental Contamination and Toxicology.  
540 [https://doi.org/10.1007/398\\_2020\\_51](https://doi.org/10.1007/398_2020_51)
- 541 Andreu, V., Gimeno-García, E., Pascual, J.A., Vazquez-Roig, P., Picó, Y., 2016. Presence of  
542 pharmaceuticals and heavy metals in the waters of a Mediterranean coastal wetland: potential

543 interactions and the influence of the environment. *Science of the Total Environment* 540, 278-  
544 286. <https://doi.org/10.1016/j.scitotenv.2015.08.007>

545 Arab, K., Steghens, J.-P., 2004. Plasma lipid hydroperoxides measurement by an automated xylenol  
546 orange method. *Analytical Biochemistry* 325, 158–163.  
547 <https://doi.org/10.1016/j.ab.2003.10.022>

548 Apeti, D.A., Lauenstein, G.G., Evans, D.W., 2012. Recent Status of Total Mercury and Methyl Mercury  
549 in the Coastal Waters of the Northern Gulf of Mexico Using Oysters and Sediments from  
550 NOAA’s Mussel Watch Program. *Marine Pollution Bulletin* 64 (11): 2399–2408.  
551 <https://doi.org/10.1016/j.marpolbul.2012.08.006>

552 Au, D.W.T., 2004. The application of histo-cytopathological biomarkers in marine pollution  
553 monitoring: a review. *Marine Pollution Bulletin* 48, 817-834.  
554 <https://doi.org/10.1016/j.marpolbul.2004.02.032>

555 Beauvais-Flück, R., Gimbert, F., Méhault, O., Cosio, C., 2017. Trophic fate of inorganic and  
556 methylmercury in a macrophyte-chironomid food chain. *Journal of Hazardous Materials* 338,  
557 140–147. <https://doi.org/10.1016/j.jhazmat.2017.05.028>

558 Beer, R.F., Sizer, I.W., 1952. A spectrophotometric method for measuring the breakdown of hydrogen  
559 peroxide by catalase. *J Biol Chem* 195 (1), 133–40. PMID: 14938361

560 Biagianti-Risbourg, S., 1957. Les perturbations (ultra)structurales du foie des poissons utilisées  
561 comme biomarqueurs de la qualité sanitaire des milieux aquatiques. In: Lagadic Amiard, J.C.,  
562 Caquet, T., And Ramande, F., (EDS), Utilisation de biomarqueurs en écotoxicologie, aspects  
563 fondamentaux. Masson Pub., Paris, 355-391

564 Bielen, A., Bošnjak, I., Sepčić, K., 2016. Differences in tolerance to anthropogenic stress between  
565 invasive and native bivalves. *Sci. Total Environ.* 543 (Part A), 449-459.  
566 <https://doi.org/10.1016/j.scitotenv.2015.11.049>

567 Bigas, M., Durfort, M., Poquet, M., 2006. Cytological response of hemocytes in the European flat  
568 oyster, *Ostrea edulis*, experimentally exposed to mercury. *BioMetals* 19, 659–673.  
569 <https://doi.org/10.1007/s10534-006-9003-5>

570 Binelli, A., Della Torre, C., Magni, S., Parolini, M., 2015. Does zebra mussel (*Dreissena polymorpha*)  
571 represent the freshwater counterpart of *Mytilus* in ecotoxicological studies? A critical review.  
572 *Environmental Pollution* 196, 386–403. <https://doi.org/10.1016/j.envpol.2014.10.023>

573 Brandts, I., Teles, M., Gonçalves, A.P., Barreto, A., Franco-Martinez, L., Tvarijonaviciute, A., Martins,  
574 M.A., Soares, A.M.V.M., Tort, L., Oliveira, M., 2018. Effects of nanoplastics on *Mytilus*  
575 *galloprovincialis* after individual and combined exposure with carbamazepine. *Science of The*  
576 *Total Environment* 643, 775–784. <https://doi.org/10.1016/j.scitotenv.2018.06.257>

577 Bravo, A.G., Cosio, C., Amouroux, D., Zopfi, J., Chevalley, P.-A., Spangenberg, J.E., Ungureanu, V.-G.,  
578 Dominik, J., 2014. Extremely elevated methylmercury levels in water, sediment and organisms  
579 in a Romanian reservoir affected by release of mercury from a chlor-alkali plant. *Water*  
580 *Research* 49, 391–405. <https://doi.org/10.1016/j.watres.2013.10.024>

581 Brinke B., 2017. Toxicogenomics in environmental science. In *in vitro Environmental Toxicology –*  
582 *Concepts, Application and Assessment*, Reifferscheid et al, Eds Springer International  
583 Publishing, 159.

584 Calder, P.C., 2006. Branched-Chain Amino Acids and Immunity. *The Journal of Nutrition* 136, 288S-  
585 293S. <https://doi.org/10.1093/jn/136.1.288S>

586 Calisto, V., Bahlmann, A., Schneider, R.J., Esteves, V.I., 2011. Application of an ELISA to the  
587 quantification of carbamazepine in ground, surface and wastewaters and validation with LC-  
588 MS/MS. *Chemosphere* 84 (11): 1708-15. <https://doi.org/10.1016/j.chemosphere.2011.04.072>

589 Cappello, T., Maisano, M., D’Agata, A., Natalotto, A., Mauceri, A., Fasulo, S., 2013. Effects of  
590 environmental pollution in caged mussels (*Mytilus galloprovincialis*). *Marine Environmental*  
591 *Research* 91, 52–60. <https://doi.org/10.1016/j.marenvres.2012.12.010>

592 Cardoso, P.G., Grilo, T.F., Pereira, E., Duarte, A.C., Pardal, M.A., 2013. « Mercury Bioaccumulation and  
593 Decontamination Kinetics in the Edible Cockle *Cerastoderma Edule* ». *Chemosphere* 90 (6):  
594 1854-59. <https://doi.org/10.1016/j.chemosphere.2012.10.005>

595 Celiz, M.D., Perez, S., Barcelo, D., Aga, D.S., 2009. Trace Analysis of Polar Pharmaceuticals in  
596 Wastewater by LC-MS-MS: Comparison of Membrane Bioreactor and Activated Sludge  
597 Systems. *Journal of Chromatographic Science* 47, 19–25.  
598 <https://doi.org/10.1093/chromsci/47.1.19>

599 Chalhmi, H., Bourdineaud, J.-P., Haouas, Z., Gourves, P.-Y., Zrafi, I., Saidane-Mosbahi, D., 2016.  
600 Transcriptomic, Biochemical, and Histopathological Responses of the Clam *Ruditapes*  
601 *decussatus* from a Metal-Contaminated Tunis Lagoon. *Archives of Environmental*  
602 *Contamination and Toxicology* 70, 241–256. <https://doi.org/10.1007/s00244-015-0185-0>

603 Chen, H., Zha, J., Liang, X., Li, J., Wang, Z., 2014. Effects of the human antiepileptic drug  
604 carbamazepine on the behavior, biomarkers, and heat shock proteins in the Asian clam  
605 *Corbicula fluminea*. *Aquatic Toxicology* 155, 1–8.  
606 <https://doi.org/10.1016/j.aquatox.2014.06.001>

607 Clara, M., Strenn, B., Kreuzinger, N., 2004. Carbamazepine as a possible anthropogenic marker in the  
608 aquatic environment: investigations on the behaviour of Carbamazepine in wastewater  
609 treatment and during groundwater infiltration. *Water Research* 38, 947-954.  
610 <https://doi.org/10.1016/j.watres.2003.10.058>

611 Claveau, J., Monperrus, M., Jarry, M., Baudrimont, M., Gonzalez, P., Cavalheiro, J., Mesmer-Dudons,  
612 N., Bolliet, V., 2015. Methylmercury effects on migratory behaviour in glass eels (*Anguilla*  
613 *anguilla*): An experimental study using isotopic tracers. *Comparative Biochemistry and*  
614 *Physiology Part C: Toxicology & Pharmacology* 171, 15–27.  
615 <https://doi.org/10.1016/j.cbpc.2015.03.003>

616 Coppola, F., Almeida, Â., Henriques, B., Soares, A.M.V.M., Figueira, E., Pereira, E., Freitas, R., 2017.  
617 Biochemical impacts of Hg in *Mytilus galloprovincialis* under present and predicted warming  
618 scenarios. *Science of The Total Environment* 601–602, 1129–1138.  
619 <https://doi.org/10.1016/j.scitotenv.2017.05.201>

620 Correa, M.G., Bittencourt, L.O., Nascimento, P.C., Ferreira, R.O., Araga, W.A.B., Silva, M.C.F., Gomes-  
621 Leal, W., Fernandes, M.S., Dionizio, A., Buzalaf, M.R., Crespo-Lopez, M.E., Lima, R.R., 2020.  
622 Spinal cord neurodegeneration after inorganic mercury long-term exposure in adult rats:  
623 Ultrastructural, proteomic and biochemical damages associated with reduced neuronal  
624 density. *Ecotox Env Saf* 191, 110159. <https://doi.org/10.1016/j.ecoenv.2019.110159>

625 Daniele, G., Fieu, M., Joachim, S., Bado-Nilles, A., Beaudouin, R., Baudoin, P., James-Casas, A., Andres,  
626 S., Bonnard, M., Bonnard, I., Geffard, A., Vulliet, E., 2017. Determination of Carbamazepine and  
627 12 Degradation Products in Various Compartments of an Outdoor Aquatic Mesocosm by  
628 Reliable Analytical Methods Based on Liquid Chromatography-Tandem Mass Spectrometry.  
629 *Environmental Science and Pollution Research* 24 (20), 16893-904.  
630 <https://doi.org/10.1007/s11356-017-9297-6>

631 Dominik, J., Tagliapietra, D., Bravo, A.G., Sigovini, M., Spangenberg, J.E., Amouroux, D., Zonta, R.,  
632 2014. Mercury in the Food Chain of the Lagoon of Venice, Italy. *Marine Pollution Bulletin* 88  
633 (1–2): 194–206. <https://doi.org/10.1016/j.marpolbul.2014.09.005>

634 do Amaral, Q.D.F., Da Rosa, E., Wronski, J.G., Zuravski, L., Querol, M.V.M., dos Anjos, B., de Andrade,  
635 C.F.F., Machado, M.M., de Oliveira, L.F.S., 2019. Golden mussel (*Limnoperna fortunei*) as a  
636 bioindicator in aquatic environments contaminated with mercury: Cytotoxic and genotoxic  
637 aspects. *Science of The Total Environment* 675, 343–353.  
638 <https://doi.org/10.1016/j.scitotenv.2019.04.108>

639 ETOX, 2011. "Datenbank für ökotoxikologische Wirkungsdaten und Qualitätsziele." from  
640 <http://webetox.uba.de/webETOX/index.do> (12/10/2021)

641 Faggio, C., Tsarpali, V., Dailianis, S., 2018. Mussel digestive gland as a model tissue for assessing  
642 xenobiotics: An overview. *Science of The Total Environment* 636, 220–229.  
643 <https://doi.org/10.1016/j.scitotenv.2018.04.264>

644 Ferreira, F.F., Nazari, E.M., Muller, Y.M.R., 2018. MeHg causes ultrastructural changes in  
645 mitochondria and autophagy in the spinal cord cells of chicken embryo. *J Toxicol*, 2018,  
646 8460490. <https://doi.org/10.1155/2018/8460490>

647 Franzellitti, S., Fabbri, E., 2006. Cytoprotective responses in the Mediterranean mussel exposed to  
648 Hg<sub>2</sub><sup>+</sup> and CH<sub>3</sub>Hg<sup>+</sup>. *Biochemical and Biophysical Research Communications* 351, 719–725.  
649 <https://doi.org/10.1016/j.bbrc.2006.10.089>

650 Franzellitti, S., Balbi, T., Montagna, M., Fabbri, R., Valbonesi, P., Fabbri, E., Canesi, L., 2019.  
651 Phenotypical and molecular changes induced by carbamazepine and propranolol on larval  
652 stages of *Mytilus galloprovincialis*. *Chemosphere* 234, 962–970.  
653 <https://doi.org/10.1016/j.chemosphere.2019.06.045>

654 Freitas, R., Almeida, Â., Calisto, V., Velez, C., Moreira, A., Schneider, R.J., Esteves, V.I., Wrona, F.J.,  
655 Soares, A.M.V.M., Figueira, E., 2015. How life history influences the responses of the clam  
656 *Scrobicularia plana* to the combined impacts of carbamazepine and pH decrease.  
657 *Environmental Pollution* 202, 205–214. <https://doi.org/10.1016/j.envpol.2015.03.023>

658 Gagnaire, B., Thomas-Guyon, H., Renault, T., 2004. In vitro effects of cadmium and mercury on Pacific  
659 oyster, *Crassostrea gigas* (Thunberg), haemocytes, *Fish & Shellfish Immunology*, 16 (4), 501-  
660 512. <https://doi.org/10.1016/j.fsi.2003.08.007>

661 Garaud, M., Auffan, M., Devin, S., Felten, V., Pagnout, C., Pain-Devin, S., Proux, O., Rodius, F., Sohm,  
662 B., Giamberini, L., 2016. « Integrated Assessment of Ceria Nanoparticle Impacts on the  
663 Freshwater Bivalve *Dreissena Polymorpha* ». *Nanotoxicology* 10 (7): 935-44.  
664 <https://doi.org/10.3109/17435390.2016.1146363>

665 González-Mira, A., Varó, I., Solé, M., Torreblanca, A., 2016. Drugs of environmental concern modify  
666 *Solea senegalensis* physiology and biochemistry in a temperature-dependent manner. *Environ*  
667 *Sci Pollut Res* 23, 20937–20951. <https://doi.org/10.1007/s11356-016-7293-x>

668 Hani, Y.M.I., Prud'Homme, S.M., Nuzillard, J.-M., Bonnard, I., Robert, C., Nott, K., Ronkart, S.,  
669 Dedourge-Geffard, O., Geffard, A., 2021. 1H-NMR metabolomics profiling of zebra mussel  
670 (*Dreissena polymorpha*): A field-scale monitoring tool in ecotoxicological studies.  
671 *Environmental Pollution* 270, 116048. <https://doi.org/10.1016/j.envpol.2020.116048>

672 Hare, M. F., Atchison, W. D., 1992. Comparative action of methylmercury and divalent inorganic  
673 mercury on nerve terminal and intraterminal mitochondrial membrane potentials. *J Pharmacol*  
674 *Exp Ther* 261, 166-72.

675 Huang, S.S.Y., Benskin, J.P., Chandramouli, B., Butler, H., Helbing, C.C., Cosgrove, J.R., 2016.  
676 Xenobiotics Produce Distinct Metabolomic Responses in Zebrafish Larvae ( *Danio rerio* ).  
677 *Environ. Sci. Technol.* 50, 6526–6535. <https://doi.org/10.1021/acs.est.6b01128>

678 Huang, S.S.Y., Benskin, J.P., Veldhoen, N., Chandramouli, B., Butler, H., Helbing, C.C., Cosgrove, J.R.,  
679 2017. A multi-omic approach to elucidate low-dose effects of xenobiotics in zebrafish ( *Danio*  
680 *rerio* ) larvae. *Aquatic Toxicology* 182, 102–112.  
681 <https://doi.org/10.1016/j.aquatox.2016.11.016>

682 Jacquin, L., Gandar, A., Aguirre-Smith, M., Perrault, A., Hénaff, M.L., Jong, L.D., Paris-Palacios, S.,  
683 Laffaille, P., Jean, S., 2019. High temperature aggravates the effects of pesticides in goldfish.  
684 *Ecotoxicology and Environmental Safety* 172, 255–264.  
685 <https://doi.org/10.1016/j.ecoenv.2019.01.085>

686 Jaffal, A., Betoulle, S., Biagianti-Risbourg, S., Terreau, A., Sanchez, W., Paris-Palacios, S., 2015. Heavy  
687 metal contamination and hepatic toxicological responses in brown trout (*Salmo trutta*) from  
688 the Kerguelen Islands. *Polar Research* 34, 22784. <https://doi.org/10.3402/polar.v34.22784>

689 Jaumot, J., Navarro, A., Faria, M., Barata, C., Tauler, R., Piña, B., 2015. qRT-PCR evaluation of the  
690 transcriptional response of zebra mussel to heavy metals. *BMC Genomics* 16.  
691 <https://doi.org/10.1186/s12864-015-1567-4>

692 Jiang, W., Fang, Jianguang, Gao, Y., Du, M., Fang, Jinghui, Wang, X., Li, F., Lin, F., Jiang, Z., 2019.  
693 Biomarkers responses in Manila clam, *Ruditapes philippinarum* after single and combined  
694 exposure to mercury and benzo[a]pyrene. *Comparative Biochemistry and Physiology Part C:*  
695 *Toxicology & Pharmacology* 220, 1–8. <https://doi.org/10.1016/j.cbpc.2019.02.010>

696 Kase R. 2010. Stoffdatenblattentwurf für Carbamazepin (Stand 15/02/2010; update 30/04/2010).

697 Kershaw, J.L., Hall, A.J., 2019. Mercury in cetaceans: Exposure, bioaccumulation and toxicity. *Science*  
698 *of the Total Environment* 694, 133683. <https://doi.org/10.1016/j.scitotenv.2019.133683>

699 Kovacevic, V., Simpson, A.J., Simpson, M.J., 2016. <sup>1</sup>H NMR-based metabolomics of *Daphnia magna*  
700 responses after sub-lethal exposure to triclosan, carbamazepine and ibuprofen. *Comparative*  
701 *Biochemistry and Physiology Part D: Genomics and Proteomics* 19, 199–210.  
702 <https://doi.org/10.1016/j.cbd.2016.01.004>

703 Lam, M.W., Young, C.J., Brain, R.A., Johnson, D.J., Hanson, M.A., Wilson, C.J., Richards, S.M.,  
704 Solomon, K.R., Mabury, S.A., 2004. Aquatic persistence of eight pharmaceuticals in a  
705 microcosm study. *Environmental Toxicology and Chemistry* 23(6), 1431-1440.  
706 <https://doi.org/10.1897/03-421>

707 Le Guernic, A., Sanchez, W., Bado-Nilles, A., Palluel, O., Turies, C., Chadili, E., Cavalié, I., Delahaut, L.,  
708 Adam-Guillermin, C., Porcher, J.-M., Geffard, A., Betoulle, S., Gagnaire, B., 2016. In situ effects  
709 of metal contamination from former uranium mining sites on the health of the three-spined  
710 stickleback (*Gasterosteus aculeatus*, L.). *Ecotoxicology* 25(6), 1234-59.  
711 <https://doi.org/10.1007/s10646-016-1677-z>

712 Lee, Y.H., Kang, H.-M., Kim, D.-H., Wang, M., Jeong, C.-B., Lee, J.-S., 2017a. Adverse effects of  
713 methylmercury (MeHg) on life parameters, antioxidant systems, and MAPK signaling pathways  
714 in the copepod *Tigriopus japonicus*. *Aquatic Toxicology* 184, 133–141.  
715 <https://doi.org/10.1016/j.aquatox.2017.01.010>

716 Lee, Y.H., Kim, D.-H., Kang, H.-M., Wang, M., Jeong, C.-B., Lee, J.-S., 2017b. Adverse effects of  
717 methylmercury (MeHg) on life parameters, antioxidant systems, and MAPK signaling pathways  
718 in the rotifer *Brachionus koreanus* and the copepod *Paracyclops nana*. *Aquatic Toxicology*  
719 190, 181–189. <https://doi.org/10.1016/j.aquatox.2017.07.006>

720 Liu, X., Zhang, L., You, L., Cong, M., Zhao, J., Wu, H., Li, C., Liu, D., Yu, J., 2011a. Toxicological  
721 responses to acute mercury exposure for three species of Manila clam *Ruditapes philippinarum*  
722 by NMR-based metabolomics. *Environmental Toxicology and Pharmacology* 31, 323–332.  
723 <https://doi.org/10.1016/j.etap.2010.12.003>

724 Liu, X., Zhang, L., You, L., Yu, J., Zhao, J., Li, L., Wang, Q., Li, F., Li, C., Liu, D., Wu, H., 2011b.  
725 Differential toxicological effects induced by mercury in gills from three pedigrees of Manila  
726 clam *Ruditapes philippinarum* by NMR-based metabolomics. *Ecotoxicology* 20, 177–186.  
727 <https://doi.org/10.1007/s10646-010-0569-x>

728 Louis, F., Devin, S., Giambérini, L., Potet, M., David, E., Pain-Devin, S., 2019. Energy allocation in two  
729 dreissenid species under metal stress. *Environmental Pollution* 245, 889–897.  
730 <https://doi.org/10.1016/j.envpol.2018.11.079>

731 Louis, F., Rocher, B., Barjhoux, I., Bultelle, F., Dedourge-Geffard, O., Gaillet, V., Bonnard, I., Delahaut,  
732 L., Pain-Devin, S., Geffard, A., Paris-Palacios, S., David, E., 2020. Seasonal monitoring of cellular  
733 energy metabolism in a sentinel species, *Dreissena polymorpha* (bivalve): Effect of global  
734 change? *Science of the Total Environment* 725, 138450.  
735 <https://doi.org/10.1016/j.scitotenv.2020.138450>

736 Magniez, G., Franco, A., Geffard, A., Rioult, D., Bonnard, I., Delahaut, L., Joachim, S., Daniele, G.,  
737 Vulliet, E., Porcher, J.-M., Bonnard, M., 2018. Determination of a new index of sexual maturity  
738 (ISM) in zebra mussel using flow cytometry: interest in ecotoxicology. *Environmental Science*  
739 *and Pollution Research* 25, 11252–11263. <https://doi.org/10.1007/s11356-017-9256-2>

740 Martin-Diaz, L., Franzellitti, S., Buratti, S., Valbonesi, P., Capuzzo, A., Fabbri, E., 2009. Effects of  
741 environmental concentrations of the antiepileptic drug carbamazepine on biomarkers and  
742 cAMP-mediated cell signaling in the mussel *Mytilus galloprovincialis*. *Aquatic Toxicology* 94,  
743 177–185. <https://doi.org/10.1016/j.aquatox.2009.06.015>

744 Metcalfe, C.D., Koenig, B.G., Bennie, D.T., Servos, M., Ternes, T.A., Hirsch, R., 2009. Occurrence of  
745 neutral and acidic drugs in the effluents of Canadian sewage exposure plants. *Environmental*  
746 *toxicology and chemistry* 22 (12): 2872-80. <https://doi.org/10.1897/02-469>

747 Metian, M., Pouil, S., Dupuy, C., Teyssié, J.-L., Warnau, M., Bustamante, P., 2020. Influence of food  
748 (ciliate and phytoplankton) on the trophic transfer of inorganic and methylmercury in the  
749 Pacific cupped oyster *Crassostrea gigas*. *Environmental Pollution* 257, 113503.  
750 <https://doi.org/10.1016/j.envpol.2019.113503>

751 Miao, X.-S., Yang, J.-J., Metcalfe, C.D., 2005. Carbamazepine and Its Metabolites in Wastewater and  
752 in Biosolids in a Municipal Wastewater Exposure Plant. *Environ. Sci. Technol.* 39, 7469–7475.  
753 <https://doi.org/10.1021/es050261e>

754 Minamata International Convention, 2013. <https://www.mercuryconvention.org/en> (12/10/2021)

755 Moermond, C.T.A., 2014. Environmental risk limits for pharmaceuticals. National Institute for Public  
756 Health and the Environment (Netherlands). Available at [www.rivm.nl/en](http://www.rivm.nl/en) (12/10/2021)

757 Navarro, A., Faria, M., Barata, C., Piña, B., 2011. Transcriptional response of stress genes to metal  
758 exposure in zebra mussel larvae and adults. *Environmental Pollution* 159, 100–107.  
759 <https://doi.org/10.1016/j.envpol.2010.09.018>

760 Navarro, A., Weißbach, S., Faria, M., Barata, C., Piña, B., Luckenbach, T., 2012. Abcb and Abcc  
761 transporter homologs are expressed and active in larvae and adults of zebra mussel and  
762 induced by chemical stress. *Aquatic Toxicology* 122–123, 144–152.  
763 <https://doi.org/10.1016/j.aquatox.2012.06.008>

764 Oldenkamp, R., Beusen, A.H.W., Huijbregts, M.A.J., 2019. Aquatic risks from human  
765 pharmaceuticals—modelling temporal trends of carbamazepine and ciprofloxacin at the global  
766 scale. *Environmental Research Letters* 14, 034003. <https://doi.org/10.1088/1748-9326/ab0071>

767 Oliveira, P., Almeida, Â., Calisto, V., Esteves, V.I., Schneider, R.J., Wrona, F.J., Soares, A.M.V.M.,  
768 Figueira, E., Freitas, R., 2017. Physiological and biochemical alterations induced in the mussel  
769 *Mytilus galloprovincialis* after short and long-term exposure to carbamazepine. *Water*  
770 *Research* 117, 102–114. <https://doi.org/10.1016/j.watres.2017.03.052>

771 Pain-Devin, S., Cossu-Leguille, C., Geffard, A., Giambérini, L., Jouenne, T., Minguez, L., Naudin, B.,  
772 Parant, M., Rodius, F., Rousselle, P., Tarnowska, K., Daguin-Thiébaud, C., Viard, F., Devin, S.,  
773 2014. Towards a better understanding of biomarker response in field survey: A case study in  
774 eight populations of zebra mussels. *Aquatic Toxicology* 155, 52–61.  
775 <http://dx.doi.org/10.1016/j.aquatox.2014.06.008>

776 Paoletti, F., Aldinucci, D., Mocali, A., Caparrini, A., 1986. A sensitive spectrophotometric method for  
777 the determination of superoxide dismutase activity in tissue extracts. *Anal. Biochem.*, 154 (2),  
778 pp. 536–541. [https://doi.org/10.1016/0003-2697\(86\)90026-6](https://doi.org/10.1016/0003-2697(86)90026-6)

779 Paris-Palacios, S., Biagianni-Risbourg, S., Vernet, G., 2000. Biochemical and (ultra)structural hepatic  
780 perturbations of *Brachydanio rerio* (Teleostei, Cyprinidae) exposed to two sublethal  
781 concentrations of copper sulfate. *Aquatic Toxicology* 50, 109–124.  
782 [https://doi.org/10.1016/S0166-445X\(99\)00090-9](https://doi.org/10.1016/S0166-445X(99)00090-9)

783 Paris-Palacios, S., Biagianni-Risbourg, S., Vernet, G., 2003. Metallothionein induction related to  
784 hepatic structural perturbations and antioxidative defenses in roach (*Rutilus rutilus*) exposed  
785 to the fungicide promycidone. *Biomarkers* 8 (2), 128–141.  
786 <http://doi.org/10.1080/1354750021000050511>

787 Parisi, M.G., Pirrera, J., La Corte, C., Dara, M., Parrinello, D., Cammarata, M., 2021. Effects of organic  
788 mercury on *Mytilus galloprovincialis* hemocyte function and morphology. *J Comp Physiol B*  
789 191, 143–158. <https://doi.org/10.1007/s00360-020-01306-0>

790 Prud'homme, S.M., Hani, Y.M.I., Cox, N., Lippens, G., Nuzillard, J.-M., Geffard, A., 2020. The Zebra  
791 Mussel (*Dreissena polymorpha*) as a Model Organism for Ecotoxicological Studies: A Prior 1H  
792 NMR Spectrum Interpretation of a Whole Body Extract for Metabolism Monitoring.  
793 *Metabolites* 10, 256. <https://doi.org/10.3390/metabo10060256>

794 Pytharopoulou, S., Kournoutou, G.G., Leotsinidis, M., Georgiou, C.D., Kalpaxis, D.L., 2013.  
795 Dysfunctions of the translational machinery in digestive glands of mussels exposed to mercury  
796 ions. *Aquatic Toxicology* 134–135, 23–33. <https://doi.org/10.1016/j.aquatox.2013.02.014>

797 Rana, M.N., Tangpong, J., Rahman, Md.M., 2018. Toxicodynamics of Lead, Cadmium, Mercury and  
798 Arsenic- induced kidney toxicity and exposure strategy: A mini review. *Toxicology Reports* 5,  
799 704–713. <https://doi.org/10.1016/j.toxrep.2018.05.012>

800 Rodrigo, A.P., Costa, P.M., 2017. The Role of the Cephalopod Digestive Gland in the Storage and  
801 Detoxification of Marine Pollutants. *Front. Physiol.* 8, 232.  
802 <https://doi.org/10.3389/fphys.2017.00232>

803 Sacher, F., Lange, F.T., Brauch, H.J., Blankenhorn, I., 2001. Pharmaceuticals in groundwaters:  
804 analytical methods and results of a monitoring program in Baden-Württemberg, Germany.  
805 Journal of chromatography A 938 (1-2): 199-210. [https://doi.org/10.1016/S0021-](https://doi.org/10.1016/S0021-9673(01)01266-3)  
806 [9673\(01\)01266-3](https://doi.org/10.1016/S0021-9673(01)01266-3)

807 Schmittgen, T.D., Livak, K.J., 2008. Analyzing real-time PCR data by the comparative CT method. Nat  
808 Protoc 3, 1101–1108. <https://doi.org/10.1038/nprot.2008.73>

809 Segner, H., Braunbeck, T., 1990. Qualitative and quantitative assessment of the response of milkfish  
810 *Chanos chanos*, fry to low-level copper exposure. In: Perkins, F.O., Cheng, T.C. (Eds),  
811 Pathology in Marine Science. Academic Press, San Diego, USA, 347-368.

812 Segner, H., Braunbeck, T., 1998. Cellular response profile to chemical stress. Ecotoxicology 3, 521-  
813 569.

814 Serra-Compte, A., Maulvault, A.L., Camacho, C., Álvarez-Muñoz, D., Barceló, D., Rodríguez-Mozaz, S.,  
815 Marques, A., 2018. Effects of water warming and acidification on bioconcentration,  
816 metabolization and depuration of pharmaceuticals and endocrine disrupting compounds in  
817 marine mussels (*Mytilus galloprovincialis*). Environmental Pollution 236, 824–834.  
818 <https://doi.org/10.1016/j.envpol.2018.02.018>

819 Sıkdokur, E., Belivermiş, M., Sezer, N., Pekmez, M., Bulan, Ö.K., Kılıç, Ö., 2020. Effects of microplastics  
820 and mercury on manila clam *Ruditapes philippinarum*: Feeding rate, immunomodulation,  
821 histopathology and oxidative stress. Environmental Pollution 262, 114247.  
822 <https://doi.org/10.1016/j.envpol.2020.114247>

823 Sijm, D.T.H.M., Hermens, J.L.M., 2001. Internal effect concentration: link between bioaccumulation  
824 and ecotoxicity for organic chemicals. Bioaccumulation – New Aspects and Developments. The  
825 Handbook of Environmental Chemistry (Vol. 2 Series: Reactions and Processes), vol 2J.  
826 Springer, Berlin, Heidelberg. [https://doi.org/10.1007/10503050\\_2](https://doi.org/10.1007/10503050_2)

827 Sokolova, I.M., Frederich, M., Bagwe, R., Lannig, G., Sukhotin, A.A., 2012. Energy homeostasis as an  
828 integrative tool for assessing limits of environmental stress tolerance in aquatic invertebrates.  
829 Marine Environmental Research 79, 1–15. <https://doi.org/10.1016/j.marenvres.2012.04.003>

830 Storey, J.D. and Tibshirani, R., 2003. Statistical significance for genomewide studies. Proceedings of  
831 the National Academy of Sciences, 100(16):9440-9445.  
832 <https://doi.org/10.1073/pnas.1530509100>

833 Storey, J.D., 2015. qvalue: Q-value estimation for false discovery rate control. R package version  
834 2.0.0, <http://qvalue.princeton.edu/>, <http://github.com/jdstorey/qvalue> (12/10/2021)

835 Sturn, A., Quackenbush, J., Trajanoski, Z., 2002. Genesis: cluster analysis of microarray data.  
836 *Bioinformatics* 18(1):207-8. <https://doi.org/10.1093/bioinformatics/18.1.207>

837 Takahashi, S., 2012. Molecular functions of metallothionein and its role in hematological  
838 malignancies. J Hematol Oncol 5, 41. <https://doi.org/10.1186/1756-8722-5-41>

839 Thiébaud, G., Tarayre, M., Jambon, O., Le Bris, N., Colinet, H., Renault, D., 2021. Variation of thermal  
840 plasticity for functional traits between populations of an invasive aquatic plant from two  
841 climatic regions. Hydrobiologia 848, 2077-2091. <https://doi.org/10.1007/s10750-020-04452-2>

842 Vaux, D.L., Fidler, F., Cumming, G., 2012. Replicates and repeats—what is the difference and is it  
843 significant? EMBO reports 13 (4), 291-296. <https://doi.org/10.1038/embor.2012.36>

844 Velez, C., Freitas, R., Antunes, S.C., Soares, A.M.V.M., Figueira, E., 2016. Clams sensitivity towards As  
845 and Hg: A comprehensive assessment of native and exotic species. Ecotoxicology and  
846 Environmental Safety 125, 43–54. <https://doi.org/10.1016/j.ecoenv.2015.11.030>

847 Viant, M.R., Rosenblum, E.S., Tjeerdema, R.S., 2003. NMR-Based Metabolomics: a powerful approach  
848 for characterizing the effects of environmental stressors on organism health. Environ Sci  
849 Technol 37:4982–4989. <https://doi.org/10.1021/es034281x>

850 Yang, L., Zhang, Y., Wang, F., Luo, Z., Guo, S., Strähle, U., 2020. Toxicity of mercury: Molecular  
851 evidence. Chemosphere 245, 125586. <https://doi.org/10.1016/j.chemosphere.2019.125586>

852  
853



854 **Table 1:** List of metabolic pathways significantly modulated at D7 in soft tissues of *D. polymorpha*  
 855 exposed to  $3.9 \pm 0.6 \mu\text{g}\cdot\text{L}^{-1}$  CBZ,  $280 \pm 20 \text{ ng}\cdot\text{L}^{-1}$  MeHg and CBZ+MeHg.

	<b>Impacted metabolic pathways at D7</b>	<b>p-value</b>
<b>CBZ</b>	Cysteine and methionine metabolism	0.021
<b>MeHg</b>	-	-
<b>CBZ + MeHg</b>	tRNA-aminoacyl biosynthesis	$8.4e^{-15}$
	Biosynthesis of branched chain amino acids BCAAs	$3.0e^{-6}$
	Arginine biosynthesis	$4.0e^{-5}$
	Glyoxylate and dicarboxylate metabolism	$8.7e^{-5}$
	Alanine, aspartate and glutamate metabolism	$7.1e^{-4}$
	Glycine, serine and threonine metabolism	0.001
	Galactose metabolism	0.008
	Glutathione metabolism	0.008
	Cysteine and methionine metabolism	0.013
	Arginine and proline metabolism	0.019
	Degradation of BCAAs	0.022
	Histidine metabolism	0.024
	Biosynthesis of neomycin, kanamycin and gentamicin	0.031
	Pantothenate and CoA biosynthesis	0.033
	Citrate cycle	0.037
	Pyruvate metabolism	0.044

856

857

858

859 **Table 2:** Alteration scores determined by histological and cytological observations after exposure to  
 860  $3.9\pm 0.6 \mu\text{g}\cdot\text{L}^{-1}$  CBZ,  $280\pm 20 \text{ ng}\cdot\text{L}^{-1}$  MeHg and CBZ+MeHg at D7 in gills and digestive glands of *D.*  
 861 *polymorpha*.

	Control	CBZ	MeHg	CBZ+MeHg
<b>Histology</b>				
<i>Gills</i>	0.7±0.2	0.9±0.1	2.9±0.1	2.0±0.5
<i>Digestive glands</i>	0.5±0.0	0.5±0.0	2.2±0.2	3.0±0.0
<b>Cytology of digestive cells</b>				
<i>General aspect</i>				
Healthy	83%	0%	11%	11%
Altered	11%	60%	86%	88%
Hyperactive	6%	53%	29%	19%
<i>Mitochondria</i>				
Altered	30±5%	50±20%	70±20%	60±10%
Mitochondrial	12±7%	13±8%	43±24%	34±14%
<i>Reticulum</i>				
Alteration score	0.4±0.3	1.0±0.4	1.9±0.5	2.1±0.3

862

863

864 **Figure 1:** Bioaccumulation and bioaccumulation factor (BAF L·kg<sup>-1</sup>) of CBZ (A) and MeHg (B) in *D.*  
865 *polymorpha* soft tissues at D1 (light) and D7 (dark), exposed to 3.9±0.6 µg·L<sup>-1</sup> CBZ, 280±20 ng·L<sup>-1</sup>  
866 MeHg and the co-exposure (mean±SEM, n=3 animals; \*p< 0.05 vs control).

867

868 **Figure 2:** Log-2 fold change profiles of metabolites at D1 and D7 in soft tissues of *D. polymorpha*  
869 exposed to 3.9±0.6 µg·L<sup>-1</sup> CBZ, 280±20 ng·L<sup>-1</sup> MeHg and the co-exposure vs controls (n=8 animals;  
870 \*p<0.05 and FC>1.5).

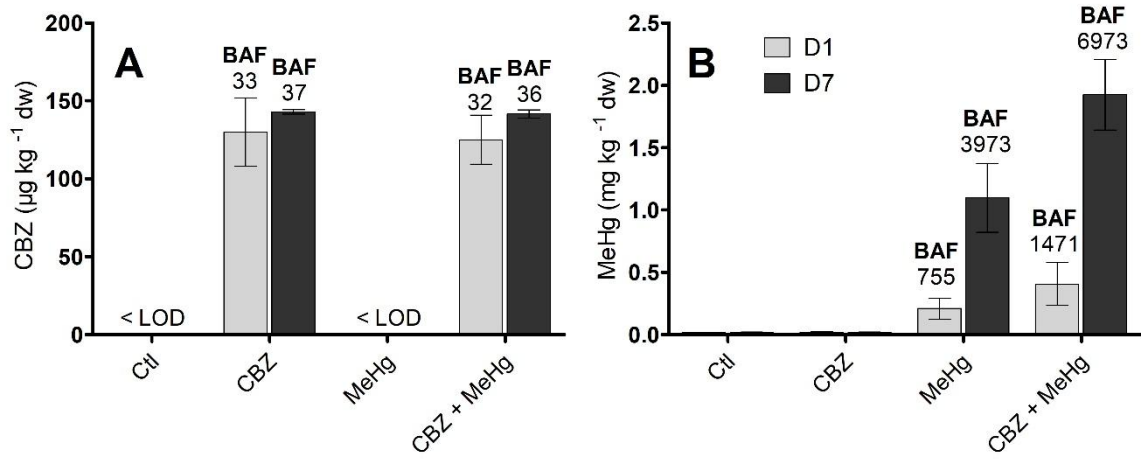
871

872 **Figure 3:** Optic (A to H) and electronic (I to L) micrographs of mussel tissues in control (A, E, I),  
873 exposed to 3.9±0.6 µg·L<sup>-1</sup> CBZ (B, F, J, K), 280±20 ng·L<sup>-1</sup> MeHg (C, G, L) and the co-exposure (D, H). Gill  
874 filaments (A to D, bar=20 µm) showing erosion of the ciliated border (e), cell vacuolization (v),  
875 necrosis (n), lysis (l), or filament with abnormal shape (\*). Fibrosis was revealed in blue by indigo in  
876 most filament gills (α) of exposed mussels. Digestive glands (E to H, bar=100 µm), showing fibrosis  
877 (α), hemocoel cell infiltration (l), atresia degenerative tubules (DT) and altered tubules with necrotic  
878 digestive cells (arrow). Digestive cells (I to L, bar=2.5 µm) showing hyperactive cells with high amount  
879 of RER and mitochondria (Mi), mostly normally conformed, and altered cells with enlargement of the  
880 nuclear inter-membrane space (eim), rare and collapsed cisternae of RER (cRER), dilated cisternae of  
881 rough endoplasmic reticulum (dRER) and altered mitochondria (aMi) which broken cristae, loss of  
882 external membrane integrity and frequent mitochondrial bodies.

883

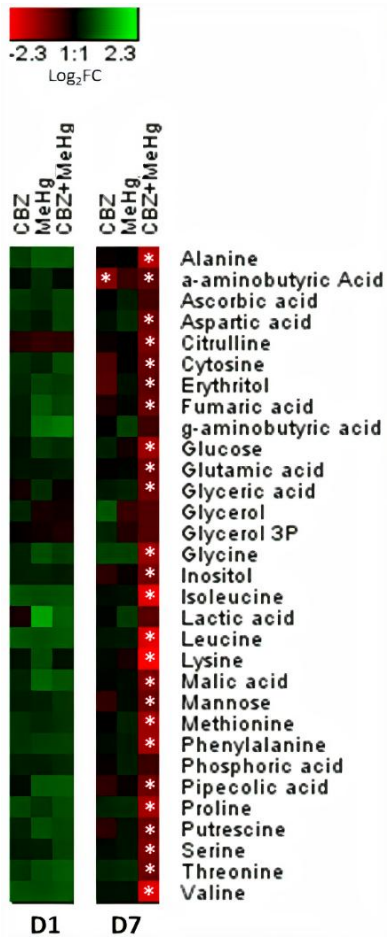
884 **Figure 4:** Relative gene expression levels of *gst* (A), *cat* (B), *sod* (C) and *mt* (D), activities of GST (E),  
885 CAT (F), SOD (G) and LOOH concentration (H) in gills and digestive glands of *D. polymorpha* at D1 and  
886 D7, exposed to control (filled, blank) 3.9±0.6 µg·L<sup>-1</sup> CBZ (green stripes), 280±20 ng·L<sup>-1</sup> MeHg (blue  
887 checkerboard) and the co-exposure (filled, yellow) (mean±SEM, n=6 to 8 animals; \*p< 0.05 vs  
888 control).

889



890  
891 Figure 1

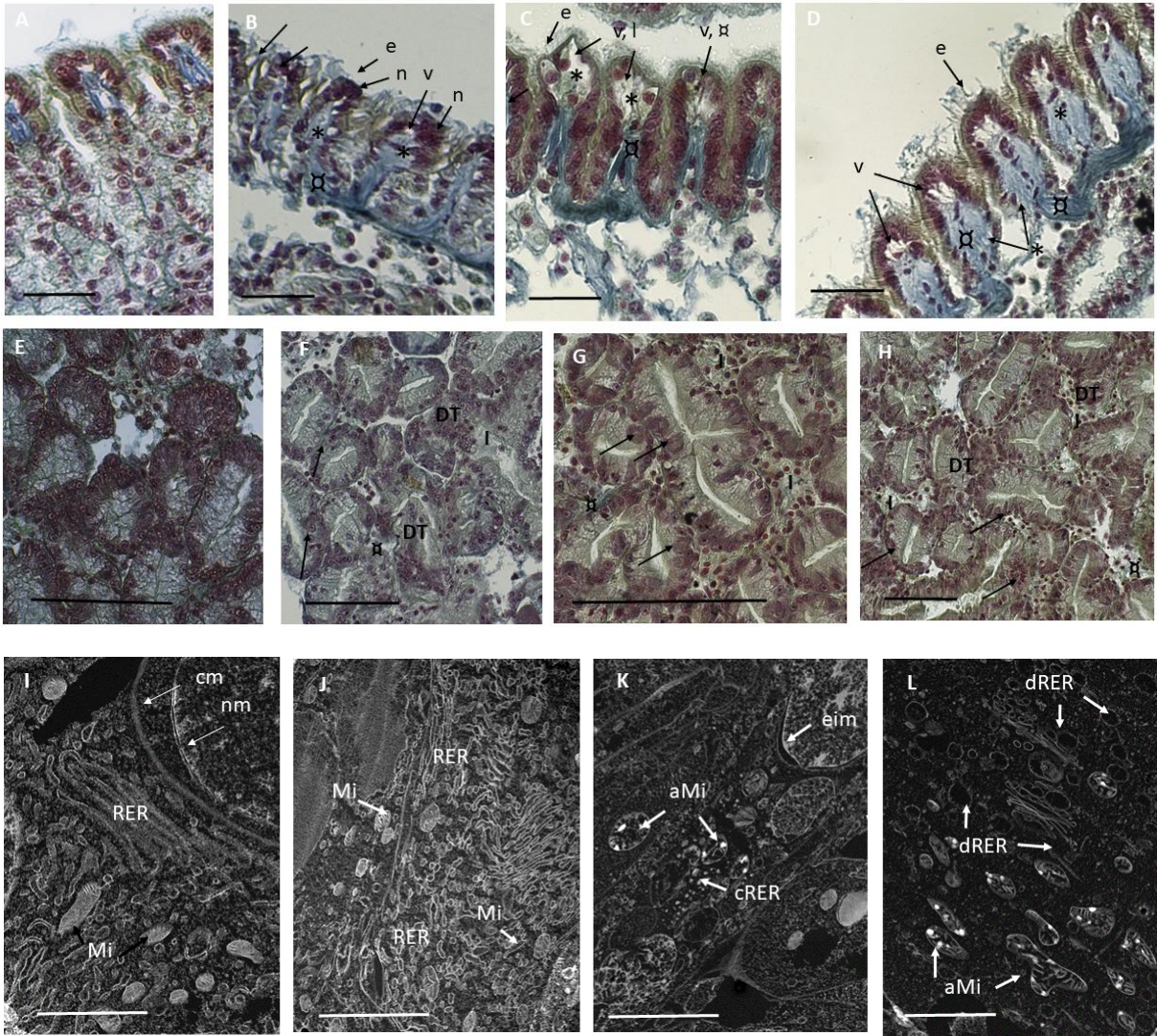
892



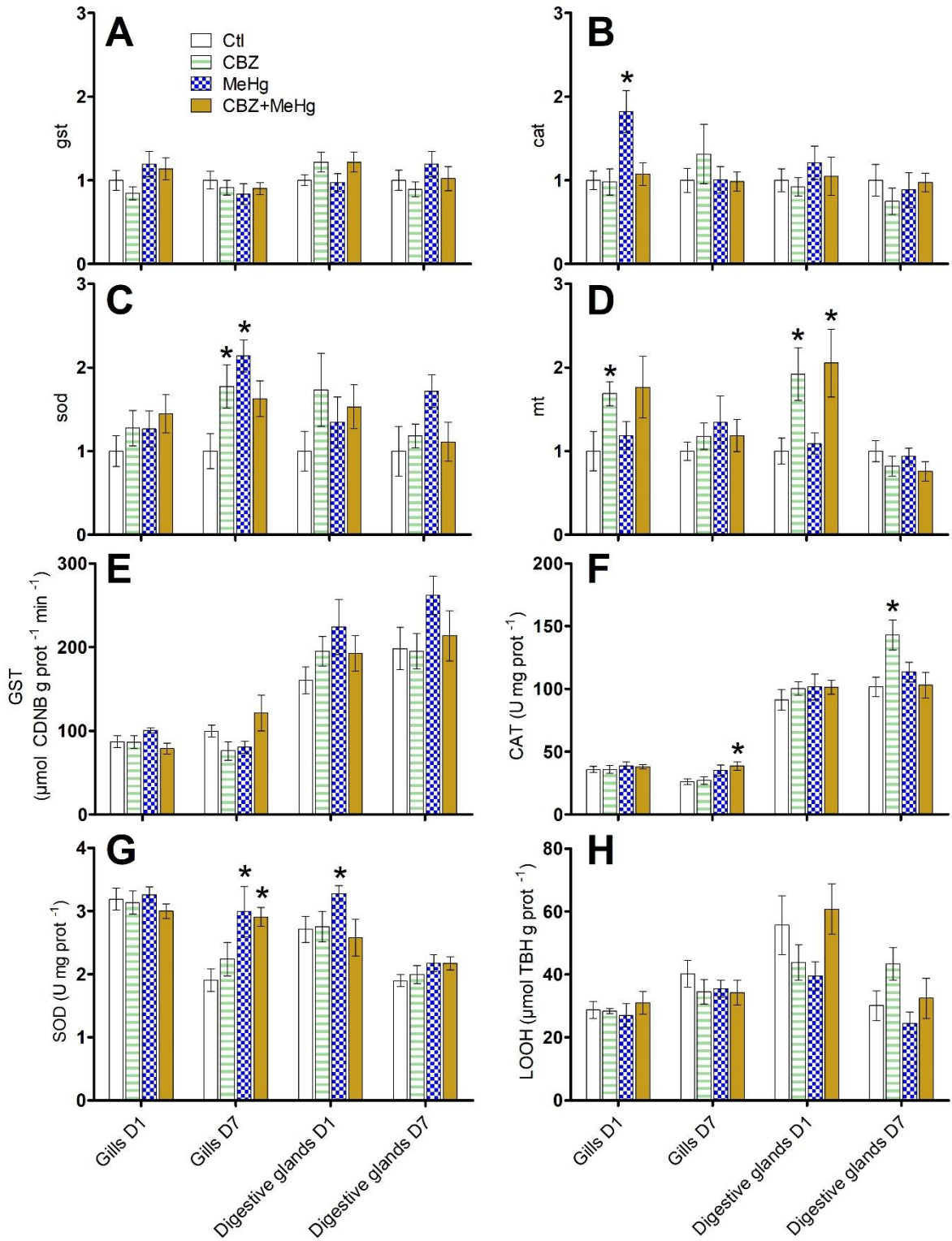
893 Figure 2

894

895



896 Figure 3  
897



898

899 Figure 4